# Thermal Imaging by Means of the Evaporograph

Gene W. McDaniel and David Z. Robinson

The development of a thermal imaging device which operates on the principle of differential evaporation (or condensation) of oil on a thin membrane is described. Section I,A summarizes the requirements of any thermal imaging method and develops the theory as applied to the particular case of the Evaporograph, emphasizing the consideration of scene temperatures near 20°C. It is shown that the greatest component of irradiance at the membrane is utilized in the evaporation of the oil layer. A presentation system which forms a visible image based on the phenomenon of light interference to detect differences in the thickness of the oil film is described. Theoretical calculations based on this system, assuming a reasonable minimum detectable thickness difference, indicate that a temperature difference of 1°C in the scene can be detected with an $f = 2$ optical system. Experimental results confirm this. The application of the Evaporograph to quantitative measurements is indicated. Section I,B describes experimental work on the three components of the Evaporograph, the infrared optical system, the transducer or cell, and the visual optical system. The two commercial models which have evolved from this work are described. These Evaporographs can detect a temperature difference of 1°C from a 20°C background and have a resolution of 10 lines per mm. Various applications are pictured and described.

## I. Theory

### A. Introduction

Thermal imaging is the process of producing a visible two-dimensional image of a scene by virtue of the differences in radiation reaching the aperture of the imaging device which apparently originate at various parts of the scene. This process depends upon the fundamental property that all bodies at temperatures above absolute zero emit thermal radiation in predictable amounts that depend upon the nature of the surface and its absolute temperature. The radiation actually reaching the imaging device is modified by other factors as will be shown.

Any thermal imaging process requires three elements:

1. An optical system which collects radiation reaching the aperture of the device and brings it to a focus to form an image of the scene.

2. A transducer which absorbs the radiation so focussed, thereby undergoing some change in its characteristics.

3. A presentation system which forms a visible image from the changes in the transducer characteristics and thus enables the eye to "see" the thermal image.

Both authors were with Baird-Atomic, Inc., Cambridge, Massachusetts; Dr. Robinson is now with the Office of the Special Assistant to the President for Science and Technology, Washington, D.C.

Received 3 July 1961.

Work done under the auspices of WADC and U.S. Signal Corps.

There are many types of thermal image-forming systems which utilize various physical properties to convert the radiation image into a visual image. An excellent summary and analysis of various image-forming systems has been made by Weihe.[1] The device to be described utilizes a transducer based on the principle known as evaporography which can be classified as an "energy proportional transducer." This means that the response of an elemental area is proportional to the total energy that has been absorbed by that area since the beginning of the imaging process.

### B. History

The principle of evaporography is one of the oldest methods of heat detection and is certainly the oldest type of thermal imaging device. Infrared radiation was first discovered by the famous English astronomer Sir W. Herschel in the sun's spectrum in the year 1800.[2] By placing a thermometer in various regions of the sun's spectrum he found that the maximum temperature was located beyond the red end of the visible spectrum. In 1840 his son, Sir J. F. W. Herschel, demonstrated the existence of absorption bands in the infrared region of the sun's spectrum.[3] Instead of a thermometer, Herschel placed a blackened piece of filter paper moistened with alcohol in the sun's spectrum. He noticed that in some places the paper became warm and the alcohol evaporated while in other areas (the absorption bands) no energy was received from the sun and the paper remained wet. This is the essential principle of evaporography.

This method of observation was forgotten for almost ninety years as people turned to bolometers and thermopiles for thermal detectors. Then, during the 1920's, Professor M. Czerny in Germany adopted this technique and developed most of the important features which are in use today.[4,5] For the filter paper Czerny substituted a thin membrane of lacquer; for an absorbing layer he used bismuth black evaporated on the membrane. In place of the alcohol he used a hydrocarbon oil. Finally, the entire system was enclosed in a housing from which the air was evacuated. Czerny used this transducer in conjunction with an infrared spectrometer to record infrared spectra.

## C. Description of the Evaporograph

The Evaporograph[6] is, therefore, a thermal imaging device which converts an infrared image into a visible image by differential evaporation or condensation of oil on a thin membrane. The operation of the Evaporograph can best be understood by referring to the simplified diagram shown in Fig. 1.

In this thermal imaging process, the first element is a germanium lens which collects the infrared radiation and brings it to a focus to form an image.

The second element of this process is the transducer or detector which consists of a very thin nitrocellulose membrane placed at the image plane (see Fig. 2). This membrane is about 0.1 micron thick; so thin that white light reflected from the front and rear surfaces of the membrane presents the first-order yellow interference color. The front surface is coated with a thin layer of gold-black which will absorb radiation. The membrane is placed within an enclosure called a cell and the air is evacuated from both sides. The rear half of the cell is lined with blotter paper moistened with a few drops of oil. This half can be heated by an electric heater which slips over the outside surface of the cell.

The irradiance at the membrane due to flux focussed thereon by the germanium lens is absorbed by the gold black, producing a heating effect. Thus, under equilibrium conditions, minute temperature differences which form a thermal reproduction of the infrared image will be present over the surface of the membrane. Now if the cell is heated, the vapor pressure of the oil will increase until the dew point is reached, at which time the oil will begin to condense upon the surface of the membrane. The condensation rate at any point is dependent upon the temperature at that point. Therefore as time progresses, an oil film will be formed whose thickness varies from point to point to form a reproduction of the thermal pattern on the membrane. Thus, the differences in infrared radiation focussed on the membrane have been converted to differences in a physical quantity: the thickness of the oil film.

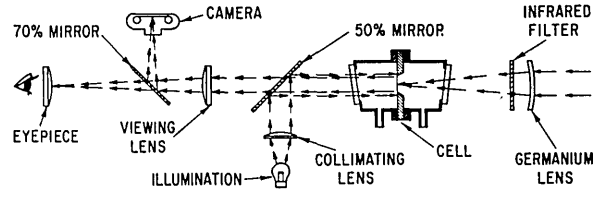


Fig. 1. Simplified schematic diagram of Evaporograph.

The third element of this process is termed the visual optical system. If the membrane is illuminated with white light the oil film pattern can be seen in different colors because of interference between reflections from the front surface of the oil film and the rear surface of the membrane. This is accomplished by a collimated beam of light from the illumination lamp reflected from the fifty percent mirror to the membrane. The useful light reflected from the membrane passes through the fifty percent mirror to the viewing lens which forms an image at the eyepiece. A seventy percent reflecting mirror placed in this beam directs light to a 35-mm camera. This allows the operator to observe and photograph the image simultaneously. Note that an infrared filter is required to prevent reflection of the illumination from the rear surface of the germanium lens back to the observer's eye.

## D. Theory of the Evaporograph

### 1. *Introduction*

The general theory of thermal imaging has been covered by several authors[1,7,8] and will not be treated in detail here. However, the results will be summarized, and then the application to the evaporographic process will be developed.

In the analysis of thermal imaging of objects at temperatures below 100°C, the importance of considering all sources which contribute to the irradiation finally reaching the transducer must be stressed. For higher temperatures many of these sources are negligible and can be disregarded.

### 2. *Power Balance at Evaporograph Membrane*

For the purpose of this analysis a simplified model of the Evaporograph cell as shown in Fig. 2 will be used. Let the membrane divide the cell into two regions which are at temperatures $T_1$ and $T_2$ and assume black-body radiation within these volumes. An optical system at temperature $T_1$ and angular aperture $2\alpha$ admits radiation from the scene to form an image on the membrane.

Consider a scene having a uniform background at a temperature $T_B$ except for an area $dA_T$ which is at a temperature $T_T$. Radiant flux from this scene passes through the intervening atmosphere at temperature $T_A$ to the entrance pupil of the optical system. Let the image on the membrane be $da_T$ at a temperature $T_{T'}$ with the surrounding area at temperature $T_{B'}$ (see Fig. 3).

The energy incident upon the membrane can be separated into two portions:

1. That portion which originates outside of the imaging device and reaches the membrane via the optical system.

2. That part which comes from within the imaging device itself.

The first portion includes the desired energy from the area $dA_T$ in the scene which is a function of the temperature $T_T$ and the spectral emittance $\epsilon_T(\lambda)$ of the body which may be dependent upon the wavelength $\lambda$. However, as mentioned earlier, when this energy reaches the entrance pupil of the optical system it will have been modified by:

1a. Energy reflected from the area, $dA_T$, which is dependent upon the spectral reflectance, $\rho_T(\lambda)$.

1b. The spectral transmittance of the atmosphere $\tau_A(\lambda)$.

1c. Energy emitted by the atmosphere at its temperature $T_A$, and spectral emittance, $\epsilon_A(\lambda)$.

The designer has no control over this radiant energy until it reaches the entrance pupil of the optical system. From this point the energy which finally reaches the membrane at $da_T$ is further modified by:

1d. The spectral transmittance $\tau_0(\lambda)$ of the optical system.

1e. Energy emitted by the optical system due to its temperature $T_1$ and spectral emittance $\epsilon_0(\lambda)$.

The second part of the energy originates within the imaging device itself and, depending upon the imaging process used, some control over this portion can be exercised. Let the spectral absorptance and emittance of the two surfaces of the membrane be $\alpha_1(\lambda)$, $\epsilon_1(\lambda)$, $\alpha_2(\lambda)$, and $\epsilon_2(\lambda)$. It will be assumed that these quantities are not dependent upon the angle of incidence. In the special case of the Evaporograph, there is also a collimated beam of light from the visual optical system which is denoted by $H_\lambda(V)$. Summarizing, the energy reaching $da_T$ from within the imaging device consists of:

2a. Black-body radiant energy from the front half of the enclosure at temperature $T_1$, excepting the solid angle subtended by the optical system.

2b. Black-body radiant energy from the rear half at temperature $T_2$.

2c. Radiant energy $H_\lambda(V)$ from the viewing system.

The energy content of the elemental area $da_T$ can also vary by:

2d. Evaporation (or condensation) of oil (denoted by $Q_4$).

2e. Radiation from the front and rear surfaces ($Q_5$).

2f. Conduction along the surface of the element to the supporting member ($Q_6$).

2g. Convection losses to the air remaining within the cell ($Q_7$).

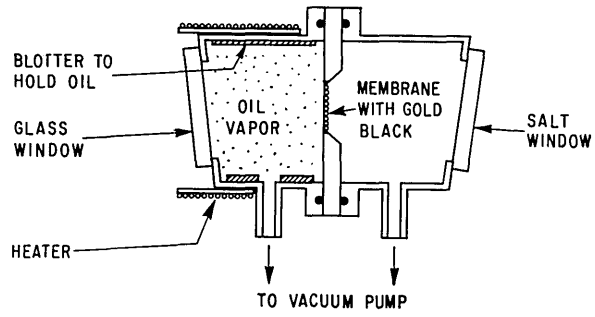


Fig. 2. Simplified schematic diagram of Evaporograph cell.

The sum of all of these energies must be zero. It must be remembered that the spectral radiant properties of these various elements are, in general, a function of the wavelength, so that integration over all wavelengths is required. Assuming that the irradiation on $dA_T$ from its surroundings is black-body radiation at a temperature $T_A$ and expressing the energies in terms of unit time, or power, one has:

$$E\,da_T\left\{\underbrace{\int_0^\infty \tau_A(\lambda)\tau_0(\lambda)\alpha_1(\lambda)[\epsilon_T(\lambda)W_\lambda(T_T)+\rho_T(\lambda)W_\lambda(T_A)]d\lambda}_{(1)}\right.$$
$$\left.+\underbrace{\int_0^\infty \tau_0(\lambda)\alpha_1(\lambda)\epsilon_A(\lambda)W_\lambda(T_A)d\lambda}_{(2)}+\underbrace{\frac{1}{\pi}\int_0^\infty \epsilon_0(\lambda)\alpha_1(\lambda)W_\lambda(T_1)d\lambda}_{(3)}\right\}$$
$$+\,da_T\underbrace{\left(1-\frac{E}{\pi}\right)\int_0^\infty \alpha_1(\lambda)W_\lambda(T_1)d\lambda}_{(4)}+da_T\underbrace{\int_0^\infty \alpha_2(\lambda)W_\lambda(T_2)d\lambda}_{(5)}$$
$$+\,da_T\underbrace{\int_0^\infty \alpha_2(\lambda)H_\lambda(V)d\lambda}_{(6)}+da_T\left[\underbrace{\int_0^\infty \epsilon_1(\lambda)W_\lambda(T_{T'})d\lambda}_{(7)}\right.$$
$$\left.+\int_0^\infty \epsilon_2(\lambda)W_\lambda(T_{T'})d\lambda\right]+q_4+q_6+q_7=0, \quad (1)$$

where $E=(1+4f^2)^{-1}$ and the small $q$'s indicate power. The terms of this equation are as follows: (1) is the power per unit area emitted and reflected by the area $dA_T$ in the scene; (2) represents the power radiated by the atmosphere between the scene and the viewing device; (3) is the power emitted by the optical system; (4) is the balance of the power received from the left due to the enclosure at temperature $T_1$; (5) is the power received from the right-hand hemisphere at temperature $T_2$; (6) is the power from the viewing light; (7) is the power radiated by the area of the membrane $da_T$. $q_4$ is the power absorbed by evaporation of oil from the membrane. $q_6$ represents the power loss by conduction along the film to the supporting surface. $q_7$ is the power loss by convection from the surface element $da_T$.

Actually we are interested in the power difference received at the membrane from the image of the area $dA_T$ in the scene and an adjacent area $dA_B$ at a background temperature $T_B$. An equation equivalent to (1) can be set up for this area $dA_B$ and its image $da_B$. Note that terms (2), (3), (4), (5), and (6) will be identical for both cases. If we let $dA_T = dA_B$, which im-

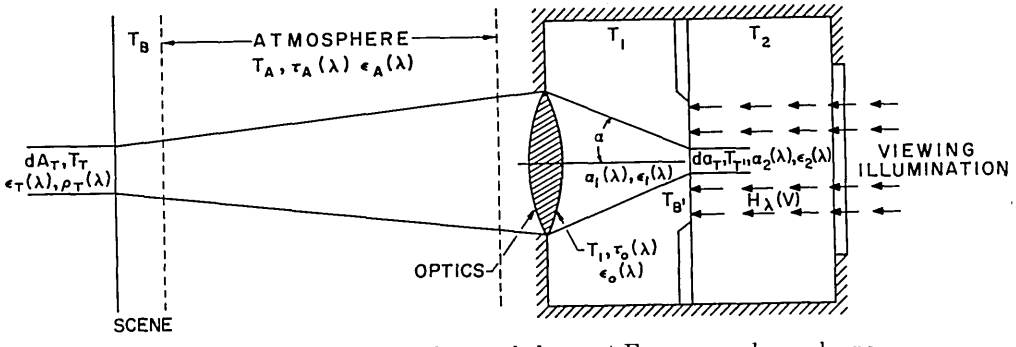


Fig. 3. Schematic diagram of power balance at Evaporograph membrane.

plies that $da_T = da_B$ and if the difference between $T_T$ and $T_B$ is sufficiently small that the spectral emittance of the surface and the spectral transmittances of the atmosphere and of the optics can be considered the same, then by subtraction one has:

$$E \int_0^\infty \tau_A(\lambda)\tau_0(\lambda)\alpha_1(\lambda)\ \epsilon_T(\lambda)\ [W_\lambda(T_T) - W_\lambda(T_B)]d\lambda = \int_0^\infty [\epsilon_1(\lambda) + \epsilon_2(\lambda)]\ [W_\lambda(T_{T'}) - W_\lambda(T_{B'})]d\lambda + \Delta q_4 + \Delta q_7. \quad (2)$$

This assumes that the power difference lost by conduction is negligible. Let us further assume that $T_T$ does not differ appreciably from $T_B$; that is,

$$T_T = T_B + \Delta T \text{ where } \Delta T \ll T_B.$$

Also let us define mean values of the various transmittances, absorptances, and emittances according to the spectral distribution of the radiation concerned; viz.,

$$\tau_A = \frac{\int_0^\infty \tau_A(\lambda)W_\lambda(T_T)d\lambda}{\int_0^\infty W_\lambda(T_T)d\lambda}. \quad (3)$$

Then, substituting these values in Eq. (2), remembering that $\int_0^\infty W_\lambda(T_B)d\lambda = \sigma T_B^4$ where $\sigma$ is the Stefan-Boltzmann constant, and neglecting terms of higher order, one obtains:

$$4\ E\tau_A\tau_0\alpha_1\epsilon_T\sigma T_B^3\ \Delta T = 4(\epsilon_1 + \epsilon_2)\sigma T_{B'}^3\ \Delta T' + \Delta q_4 + \Delta q_7$$

or, solving for $\Delta T'$,

$$\Delta T' = \frac{4E\tau_A\tau_0\alpha_1\epsilon_T\sigma T_B^3\Delta T - \Delta q_4 - \Delta q_7}{4\ (\epsilon_1 + \epsilon_2)\sigma T_{B'}^3}. \quad (4)$$

Equation (4) shows that $\Delta T'$ varies directly with the optical efficiency $E$, the transmittances of the atmosphere, $\tau_A$, and of the optical system, $\tau_0$, the emittance of the scene, $\epsilon_T$, and the absorptance of the tranducer, $\alpha_1$. It can also be increased by minimizing $\Delta q_4$ and $\Delta q_7$, and varies inversely with the transducer emittances, $\epsilon_1$ and $\epsilon_2$, and the transducer temperature, $T_{B'}$. If $\Delta q_4$ and $\Delta q_7$ are set equal to zero, one has the general equation for any thermal imaging device in which the losses due to sidewise conduction and convection are negligible.

Solving Eq. (4) for $\Delta T$ yields:

$$\Delta T = \frac{4(\epsilon_1 + \epsilon_2)\sigma T_{B'}^3\ \Delta T' + \Delta q_4 + \Delta q_7}{4E\ \tau_A\tau_0\alpha_1\epsilon_T\sigma T_B^3}. \quad (5)$$

Thus, if the convection loss, $\Delta q_7$, the power difference, $\Delta q_4$, required to evaporate a minimum perceptible thickness of oil, and the temperature rise, $\Delta T'$, are known, the minimum detectable temperature difference, $\Delta T$, in the scene can be obtained.

### 3. *Theoretical Sensitivity*

Thus far the equations derived have considered the power distribution between the membrane and its environment under equilibrium conditions. As pointed out, the analysis is of a general nature and could be applied to any thermal imaging device with slight modifications. Consider now the specific case of the Evaporograph. This is an "Energy Proportional Transducer," which means that the response is proportional to the total energy that has been received since the imaging process was started. Suppose that an oil film is formed on the membrane and then the shutter is opened to admit radiation from the scene. What is the smallest radiation difference that can be detected in a reasonable time interval by the resulting change in oil film?

Of the total energy $Q$ admitted by the optical system, only a portion is absorbed, the remainder being reflected or transmitted by the absorbing layer on the membrane. Harris[9] indicates that an "80% layer," i.e., one that absorbs 80% of the incident energy ($\alpha_1 = 0.8$) has the greatest efficiency.

This absorbed energy is dissipated as follows: (1) heating the absorbing layer ($Q_1$), (2) heating the membrane ($Q_2$), (3) heating the oil film ($Q_3$), (4) evaporating a portion of the oil film ($Q_4$), (5) reradiation losses ($Q_5$), (6) conduction losses ($Q_6$), and (7) convection losses ($Q_7$). These may be combined and expressed in terms of unit area as:

$$Q' = \int_0^\infty \alpha_1(\lambda) H_\lambda \Delta t d\lambda = Q_1 + Q_2 + Q_3 + Q_4 + Q_5 + Q_6 + Q_7,$$

where $H_\lambda$ is the spectral irradiance falling on the absorbing layer and $\Delta t$ is the time interval during which this irradiance has been present. It will be assumed that the conduction losses $Q_6$ are negligible.

Then under the proper conditions, the oil film on an elemental area, $da_B$, of the background will remain constant, while the oil film on the area $da_T$ will evaporate to form a detectable thickness difference in a time interval $\Delta t$. To evaporate this oil thickness, the temperature of the area $da_T$ must be raised an amount $\Delta T'$ above the temperature of the surrounding area. The energy required to produce and maintain this temperature increase is, for unit area:

$$Q' = (S_1\delta_1 d_1 + S_2\delta_2 d_2 + S_3\delta_3 d_3)\ \Delta T' + Q_4 + Q_5 + Q_7,$$

where

$S_1$ = specific heat of absorbing layer
$S_2$ = specific heat of membrane
$S_3$ = specific heat of oil
$\delta_1$ = density of absorbing layer
$\delta_2$ = density of membrane
$\delta_3$ = density of oil
$d_1$ = thickness of absorbing layer
$d_2$ = thickness of membrane
$d_3$ = thickness of oil.

The difference in the reradiation losses, $Q_5$, between the areas $da_T$ and $da_B$ is

$$Q_5 = (\epsilon_1 + \epsilon_2)\sigma T_{T'}{}^4\ \Delta t - (\epsilon_1 + \epsilon_2)\sigma T_{B'}{}^4\ \Delta t,$$

where $\epsilon_1$ and $\epsilon_2$ are mean values as expressed by Eq. (3) and $\Delta t$ is the time interval. In particular, if $T_{T'} = T_{B'} + \Delta T'$ and $\epsilon_1 = \epsilon_2 = 0.8$,

$$Q_5 = 1.6\sigma\ \Delta t\ [(T_{B'} \times \Delta T')^4 - T_{B'}{}^4] \approx 6.4\sigma T_{B'}{}^3\ \Delta T'\ \Delta t.$$

By substitution

$$Q' = (S_1\delta_1 d_1 + S_2\delta_2 d_2 + S_3\delta_3 d_3)\ \Delta T' + 6.4\sigma T_{B'}{}^3 \Delta T' \Delta t + Q_4 + Q_7. \quad (6)$$

The first bracket can be calculated as soon as the temperature rise $\Delta T'$ is known; also, the second term can be evaluated if $T_{B'}$ and $\Delta T'$ are known. $Q_7$ can be estimated if $\Delta T'$ and the partial pressure of the air are known. The term $Q_4$ which represents the energy required to evaporate the minimum detectable change in oil film thickness in a reasonable time remains. This term depends upon the physical constants of the oil and the thickness change required.

The value of $Q_4$ can be obtained as follows. First, from simple theory, the heat required is simply the mass evaporated per unit area multiplied by the latent heat of evaporation, or:

$$Q_4 = \Delta d\ \delta_3\ L, \quad (7)$$

where

$\Delta d$ = the thickness change required
$L$ = the heat of evaporation (cal/gm)

and the equation is written for unit area.

The temperature rise can be found as follows: Since the membrane is located in an evacuated chamber and is initially in equilibrium with the vapor pressure of the oil, the number of molecules striking a unit area per second, and hence the mass, can be calculated from kinetic theory. It is found to be[10,11]:

$$m(T_{B'}) = \theta\ (M/2\pi R T_{B'})^{1/2},$$

where

$\theta$ = vapor pressure
$M$ = molecular weight
$R$ = gas constant.

Since the film is in equilibrium with its vapor, this expression must also represent the amount of oil evaporating per square centimeter per second. Now, if the temperature of the material is raised by $\Delta T'$, there will be an excess amount of material leaving the surface, expressed by:

$$\Delta m = m(T_{B'} + \Delta T') - m(T_{B'}) = \left(\frac{M}{2\pi R}\right)^{1/2} \Delta T' \frac{\partial}{\partial T_{B'}} \frac{\theta}{\sqrt{T_{B'}}}.$$

Then,

$$Q_4 = \Delta m\ \Delta t\ L = L\ \Delta t\ \Delta T' \left(\frac{M}{2\pi R}\right)^{1/2} \frac{\partial}{\partial T_{B'}} \frac{\theta}{\sqrt{T_{B'}}}. \quad (8)$$

If $\theta$ is measured in millimeters of mercury, then (8) becomes:

$$Q_4 = 5.84 \times 10^{-2}\ \Delta t\ \Delta T' L \sqrt{M} \frac{\partial}{\partial T_{B'}} \frac{\theta}{\sqrt{T_{B'}}}. \quad (9)$$

Equation (9) is that derived by Czerny.[4]

This result can be carried further. The evaluation of $\partial/\partial T_{B'} = \theta/\sqrt{T_{B'}}$ can be accomplished by using the Clapeyron-Clausius[12] equation

$$\frac{\partial \theta}{\partial T_{B'}} = \frac{\theta L M}{R T_{B'}{}^2}, \quad (10)$$

where $M$ is the molecular weight and $L$ is the heat of evaporation per gram. Performing the indicated differentiation and substituting from (10) yields:

$$\frac{\partial}{\partial T_{B'}} \frac{\theta}{\sqrt{T_{B'}}} = \frac{\theta(2LM - RT_{B'})}{2RT_{B'}{}^{5/2}}. \quad (11)$$

Substituting this value in Eq. (9)

$$Q_4 = 2.92 \times 10^{-2} L\sqrt{M}\ \theta \Delta T' \Delta t (2LM - RT_{B'})/RT_{B'}{}^{5/2}. \quad (12)$$

By combining Eqs. (12) and (7) one obtains an expression for the increase in temperature $\Delta T'$ required to change the oil film thickness an amount $\Delta d$ in a time interval $\Delta t$. This is found to be:

$$\Delta T' = \frac{R\Delta d\,\delta_3 T'_{B'}{}^{5/2}}{2.92 \times 10^{-2}\,\Delta t\sqrt{M}\,\theta\,(2LM - RT_{B'})} \cdot \quad (13)$$

If the minimum perceptible thickness change $\Delta d$ and the physical constants $L$ and $M$ of the oil used are known, then $\Delta T'$ can be computed and Eq. (6) evaluated to find the minimum detectable energy $Q'$.

In order to apply Eq. (13), it is necessary to know the vapor pressure of the oil at the operating temperature $T_{B'}$. It will be assumed that $T_{B'} \approx 300°K$. Since the data available do not extend to this temperature, it is necessary to extrapolate the data to this region.

It is possible to derive[12] from the Clapeyron-Clausius equation a formula relating the vapor pressure of a substance with its heat of vaporization and the temperature. This equation is of the form:

$$\ln \theta = C - \frac{a}{T}. \quad (14)$$

From this it is seen that a plot of $\ln \theta$ versus $1/T$ should be a straight line and the extrapolation can be easily accomplished.

The oils that were first used in the Evaporograph were the decanes. Table I lists the physical constants of these materials, together with the vapor pressure obtained by extrapolation.

Next, the amount of energy, $Q_7$, lost by convection to the air remaining in the cell can be estimated. Again from kinetic theory, the mass of air striking unit area per second is:

$$m_a = \theta_a(M_a/2\pi RT_{B'})^{1/2},$$

where

$M_a$ = the average molecular weight of air

$\theta_a$ = the partial pressure of air in the cell.

Taking $M_a \approx 29$, $T_{B'} = 300°K$, and $\theta_a = 10\ \mu$, the result is

$$m_a = 1.8 \times 10^{-4}\ \text{gm cm}^{-2}\ \text{sec}^{-1}.$$

If these air molecules recoil at a temperature $T_{B'} + \Delta T'$, then in ten seconds the energy lost is

$$Q_7 = 2m_a\Delta T'\Delta t k_a,$$

where $k_a$ is the specific heat of air which is 0.25 cal/gm. Substituting in the above expression gives

$$Q_7 = 9 \times 10^{-4}\Delta T'\ \text{cal cm}^{-2}. \quad (15)$$

It remains to decide on the minimum detectable thickness change under the most advantageous conditions. The membrane with its oil film is viewed by reflected light from an incandescent lamp which can be considered as a black-body source. Figure 4 shows the relation of the interference colors and the optical path differences when illuminated from such a source.

Although the details will not be given here, an analysis of the minimum perceptible color difference following the works of Kubota,[13] Brown,[14] and others has shown that the most sensitive regions are the first order gray and the first order purple. Their work shows an average value for the minimum detectable optical path difference to be 0.85 m$\mu$. However, this cannot be achieved in practice due to inhomogeneities in the membrane and oil film pattern which obscure such subtle differences. A more realistic value taken from Fig. 4 would be 25 m$\mu$.

It is now possible to compute the energy $Q'$ required to maintain the temperature difference $\Delta T'$ for each oil. The results obtained are tabulated in Table II. These results are obtained from Eq. (6) with the following assumptions:

1. The membrane alone exhibits the first-order yellow interference color which means that the optical path difference between rays reflected from the front and rear surfaces is approximately 300 m$\mu$. Assuming the index of refraction is approximately 1.5, the actual thickness is $d_2 = 100$ m$\mu = 10^{-5}$ cm.
2. The optical thickness of the oil film is approximately 280 m$\mu$. Since the index of refraction of all the oils is approximately 1.43, the actual thickness is $d_3 = 100$ m$\mu = 10^{-5}$ cm.
3. Thermal mass of absorbing layer is $1.7 \times 10^{-6}$ cal °C$^{-1}$ cm$^{-2}$.
4. $T_{B'} = 300°K$.
5. Film thickness change $\Delta d = 25/2.86 = 8.7$ m$\mu \approx 10^{-1}$ cm.
6. $\Delta t = 10$ sec, selected as a convenient time interval.

It is obvious from Table II that the greatest component of energy is $Q_4$, the energy required to evaporate the oil layer. The only other appreciable components are $Q_5$, the reradiation losses, and $Q_7$, the convection losses. Since this is true, Eq. (5) can now be used to determine $\Delta T$, the minimum detectable temperature difference in the scene under these conditions.

Assume

$$\begin{aligned} \epsilon_T &= 1 \\ \alpha_1 &= \epsilon_1 = \epsilon_2 = 0.8 \\ E &= 0.059 \text{ (for an } f = 2 \text{ optical system)} \\ \tau_A\tau_0 &= 0.8. \end{aligned}$$

The salt window on the Evaporograph cell does not transmit beyond 19 $\mu$. At temperatures near 300°K only 71% of the energy radiated is below this value. Therefore the denominator of Eq. (5) must be multiplied by 0.71 to correct for this effect. Taking values for hexadecane, which has proved to be one of the better oils, application of Eq. (5) results in

$$\Delta T = 1.8°C.$$

The best results obtained in the laboratory with an $f = 2.25$ optical system and approximately 20 sec viewing time showed a sensitivity of approximately 0.5°C.

**Table I. Physical Constants of Substituted Decanes**

| Material | Molecular weight $M$ | Density (gm/cc) $\delta_3$ | Specific heat (cal/gm) $S_3$ | Vapor pressure (mm Hg at 300° K) $\theta$ | Index of refraction | Heat of vaporization (cal/gm) $L$ |
|---|---|---|---|---|---|---|
| Dodecane | 170.33 | 0.766 | 0.500 | 0.24 | 1.422 | 86.0 |
| Tridecane | 184.36 | 0.757 | 0.489 | 0.10 | 1.426 | 85.9 |
| Tetradecane | 198.38 | 0.765 | 0.497 | 0.04 | 1.429 | 85.7 |
| Hexadecane | 226.42 | 0.773 | 0.495 | 0.008 | 1.433 | 85.6 |
| Octadecane | 254.48 | 0.757 | 0.636 | 0.001 | 1.437 | 85.3 |

**Table II. Energies Required for Minimum Detectable Thickness Difference**

| Material | $\Delta T'$(°C$\times10^{-4}$) Eq. (13) | $Q_1$ (cal cm$^{-2}$ $\times10^{-6}$) | $Q_2$ (cal cm$^{-2}$ $\times10^{-6}$) | $Q_3$ (cal cm$^{-2}$ $\times10^{-6}$) | $Q_4$ (cal cm$^{-2}$ $\times10^{-6}$) | $Q_5$ (cal cm$^{-2}$ $\times10^{-6}$) | $Q_7$ (cal cm$^{-2}$ $\times10^{-6}$) | $Q'$ Eq. (6) (cal cm$^{-2}$ $\times10^{-6}$) | $Q'$ Eq. (6) (joules cm$^{-2}$ $\times10^{-4}$) |
|---|---|---|---|---|---|---|---|---|---|
| Dodecane | 0.90 | 0.00015 | 0.0007 | 0.0003 | 66 | 0.21 | 0.08 | 66 | 2.7 |
| Tridecane | 1.9 | 0.0003 | 0.0015 | 0.0007 | 65 | 0.44 | 0.17 | 66 | 2.7 |
| Tetradecane | 4.3 | 0.0007 | 0.0034 | 0.0016 | 65.5 | 1.0 | 0.39 | 67 | 2.8 |
| Hexadecane | 17.8 | 0.003 | 0.014 | 0.0068 | 66.2 | 4.2 | 1.6 | 72 | 3 |
| Octadecane | 117 | 0.02 | 0.094 | 0.056 | 64.6 | 27.5 | 10.6 | 103 | 4.3 |

*4. Figure of Merit*

The preceding analysis has shown that the largest term in Eq. (6) is $Q_4$, the energy required to evaporate the oil film. It is possible then to derive a figure of merit for the oil used.

The energy required to evaporate one centimeter of oil from a square centimeter of membrane surface is simply the heat of vaporization times the density of the oil. To obtain the energy required to evaporate an optical thickness of one centimeter, it is necessary to divide this value by the index of refraction. Thus,

$$\mathfrak{M} = \frac{L\delta_3}{n}, \tag{16}$$

where $\mathfrak{M}$ is the "figure of merit" and $n$ is the index of refraction.

For the greatest sensitivity, this figure should be as small as possible. Selection of suitable oils can be guided by application of this figure of merit. Table III lists the figure for various materials. The exact choice of material will be influenced by other factors such as the effect of the oil on the membrane material, the ability to "wet" the membrane and form a continuous film, and the exact vapor pressure, which should be from 0.01 to 0.1 mm of mercury. Examination of Table III indicates that the tetramethyl siloxane polymers should result in better performance than the straight chain hydrocarbons. Those with suitable vapor pressures are the pentamer through octamer. An attempt was made to obtain these materials. Unfortunately, only crude fractions are available which are actually mixtures fractionated to give a certain viscosity. They are known as the Dow-Corning silicone 200 fluids. The viscosity of the pure materials ranged from 2.06 to 3.88 centistokes. Therefore, the mixture of 3 centistoke viscosity was obtained and has been used in later work. This material also has the advantage of a very low freezing point (−59°C) and therefore does not freeze on the membrane when operated in cold ambient conditions as do the hydrocarbons.

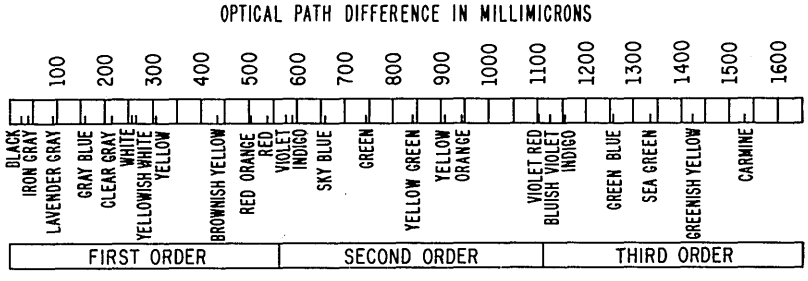


Fig. 4. Relation between optical path difference and interference colors.

**Table III. Figure of Merit for Various Materials**

| Material | Figure of merit |
|---|---|
| Dodecane | 45 |
| Tridecane | 44 |
| Tetradecane | 41 |
| Hexadecane | 43 |
| Octadecane | 43 |
| d-Camphor | 51.9 |
| Tetramethyl siloxane polymers | |
| Trimer | 27.7 |
| Tetramer | 23.6 |
| Pentamer | 20.2 |
| Hexamer | 17.9 |
| Octamer | 17.4 |

*5. Quantitative Measurements*

Equation (13) implies that, within limits, the thickness change in the oil layer is proportional to the temperature rise of a unit area of the membrane, or

$$\Delta d \propto \Delta T'.$$

For given operating conditions $\Delta T'$ can be related to the corresponding change in scene temperature $\Delta T$. Thus, it is possible to make quantitative measurements of scene temperatures. However, such measurements are difficult because there is no simple direct method of determining $\Delta d$. Also, in practice this problem is complicated by variations in the membrane from point to point. Of the various methods tested, the most accurate results have been obtained with the photographic method which will be briefly described.

As in the foregoing analysis it is assumed that the major portion of the energy entering or leaving a unit area on the membrane is utilized to evaporate or condense the oil film. Thus, one can write:

$$\Delta X_n = A_n \Delta t, \tag{17}$$

where

$\Delta X_n$ = change in oil film thickness at point $n$
$\Delta t$ = time required to produce this change
$A_n$ = a constant for any particular point.

This linear relation of film thickness with time has been verified experimentally by using monochromatic illumination and determining the film thickness by standard interferometric methods.

The system parameters can be eliminated by use of a reference source in the field of view whose emissivity is known, or is the same as that of the surface whose temperature is to be determined.

The constant $A_n$ can be expressed in terms of the radiant emittance of the scene and system parameters. For the point at which the reference source is imaged, one can write:

$$X_0 - X_R = KW_R \Delta t, \tag{18}$$

where

$X_0$ = the film thickness at time $t = 0$
$X_R$ = the film thickness after time $\Delta t$
$W_R$ = the radiant emittance of the reference source
$K$ = a constant, positive for evaporation; negative for condensation.

Now, if the instrument shutter is closed, the membrane will receive radiation equivalent to the ambient temperature of the cell, and a second equation can be written:

$$X_0 - X_{CR} = KW_{CR} \Delta t, \tag{19}$$

where $X_{CR}$ is the film thickness at the reference image point after time $\Delta t$ and $W_{CR}$ is the equivalent radiant emittance corresponding to ambient temperature $T_C$. Subtracting (19) from (18) and rearranging, one obtains

$$(W_R - W_{CR})\Delta t = K'(X_{CR} - X_R). \tag{20}$$

Similarly, for the image point of the desired object in the scene

$$(W_T - W_{CT})\Delta t = k'(X_{CT} - X_T). \tag{21}$$

If the film thicknesses can be determined, then all the values of (20) are known except K′. Substituting this value in (21) allows the computation of $W_T$ from which the temperature can be determined.

It is known that if monochromatic illumination is employed, the intensity of the reflected light will go through maxima and minima as the film thickness varies. If this reflected light is photographed on black and white film, the resulting optical density on the image will also vary from a maximum to a minimum. However, it has also been found that if white illumination is used and the images are photographed in color, similar changes in "density" readings of the processed film can be obtained if a color-sensitive densitometer is used. Figure 5 shows the variation in density units as the oil film condenses. Note that there are two linear regions on the density versus condensation time (film thickness) curve. In these regions, the film thickness can be expressed by:

$$X = K_1 D + K_2,$$

where $D$ = density. Then Eqs. (20) and (21) can be rewritten as:

$$(W_R - W_{CR})\Delta t = K_1(D_{CR} - D_R) \tag{22}$$

and

$$(W_T - W_{CT})\Delta t = K_1(D_{CT} - D_T). \tag{23}$$

Therefore, if photographs are chosen in which the densities of all of the desired image points are within one or the other of these linear regions, then Eqs. (22) and (23) can be applied directly to determine $W_T$ and from this the temperature can be computed.* *see p. 319*

(* If the densities do not lie in these linear regions, extrapolation can be employed. Also, in practice, the membrane thickness is never uniform over the entire surface. Hence a correction must be made for this condition. Methods for this have been developed, but will not be described here.)

## II. Experiments and Applications

### A. Experimental Work

*1. Introduction*

Much experimental work has been done on the various components of the Evaporograph guided by the theory which has been developed and set forth in Eqs. (6) and (13). This work can be divided into three portions, each of which pertains to one component of the thermal imaging process, i.e., (1) the infrared optical system, (2) the transducer or Evaporograph cell, and (3) the presentation system.

*2. Infrared Optical System*

As shown in Eq. (4) the temperature difference developed at the membrane is directly proportional to the efficiency of the optical system. Reflecting optical systems of the Newtonian and a modified Cassegranian type have been used. These systems have the advantage of freedom from chromatic aberration. However, because of mechanical limitations, they are necessarily of long focal length, greater than twenty centimeters. This restricts the field of view and results in a telescopic-type optical system.

Refracting optical systems using a germanium lens have also been used. Such a system can be made of relatively short focal length with the resulting wide field of view. They have the disadvantages of restricting the imaging device to wavelengths within the transmission band of the lens material, and also introduce chromatic aberration. In addition, an infrared filter must be placed in back of the lens to prevent reflection of the illumination from the visual optical system by the mirrorlike surface of the lens.

Each of these optical systems performed as expected.

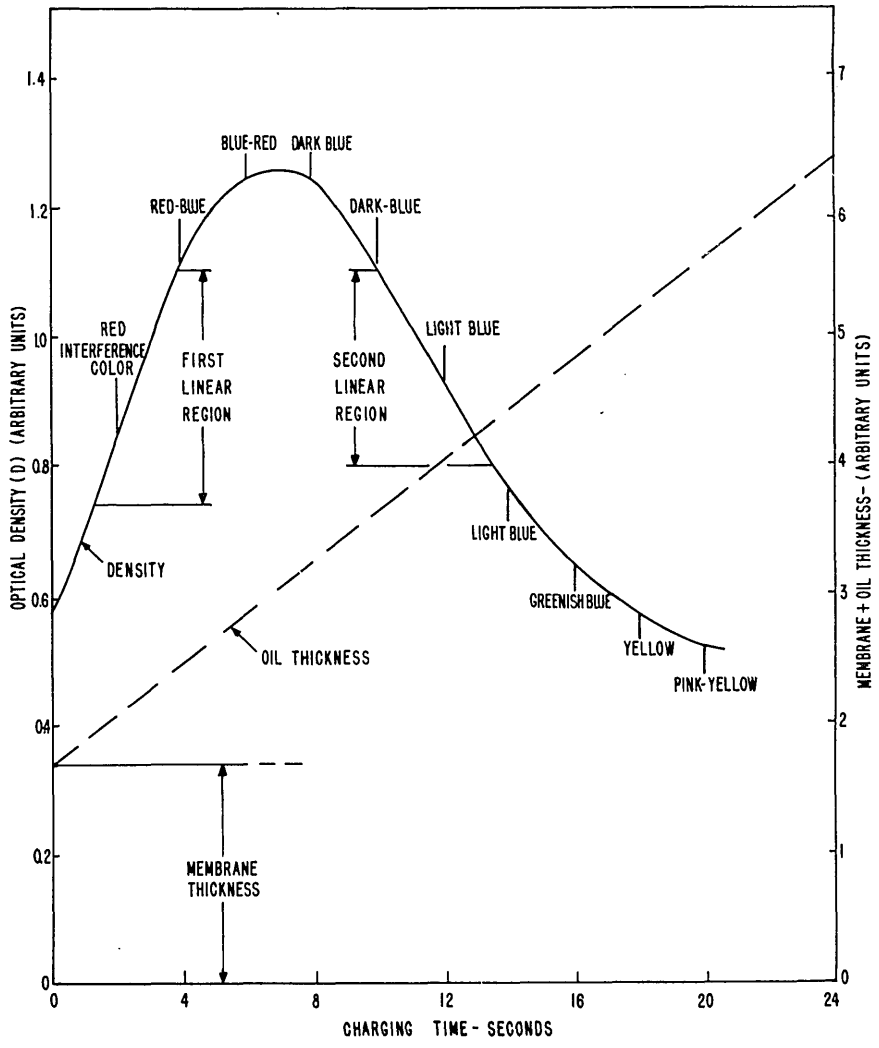


Fig 5. Oil film thickness and photographic density as a function of condensation time. (White light and color film.)

The use of any one of them will be dictated by the needs of a particular application.

### 3. *Transducer or Evaporograph Cell*

The Evaporograph cell depends upon three components: (a) the supporting layer or membrane, (b) the absorbing layer, and (c) the active material.

The supporting membrane must be a very thin uniform sheet of material with considerable strength and free from pin holes. The sheet should be approximately 0.1 $\mu$ thick. Various materials have been used for these films. The ones found most useful are listed below:

1. Amylacetate.
2. Polyvinal formal in dioxane or ethylene dichloride.
3. Polystyrene or benzene solution of Resogloz.
4. Nitrocellulose in acetone.

The films are usually formed by flotation on water, as described by Czerny,[15] Harris,[16] and others. The nitrocellulose membranes have proved to be most satisfactory and are in general use.

Experiments have also been made with aluminum oxide membranes, following the methods described by Hass[17] and Strohmaier.[18] These membranes have the advantage of very uniform thickness which is easily controllable. They have the disadvantages of reproducing the surface finish of the aluminum film which must, therefore, be of optical quality, and are somewhat more brittle than the nitrocellulose membranes. In addition, it was found to be very difficult to deposit the active material on the surface of the aluminum oxide in a uniform continuous film.

### 4. *The Absorbing Layer*

The absorbing layer must have a high absorptivity over the infrared region to be utilized. It should have a low heat capacity and must transmit the heat distribution from its receiving surface to the supporting layer with as little loss of definition as possible.

*Gold black.* In most of our work gold black has been used as the absorbing layer, formed by the method described by Harris.[9] The gold is evaporated from a tungsten filament in an atmosphere of hydrogen at a pressure of five to ten millimeters of mercury. The deposit has a very uniform absorptivity in the region from one to fifteen microns and has low thermal mass.

*Metallic layers.* As shown by Hadley,[19] if a metallic layer is evaporated on the membrane such that the resistance per square is 189 ohms, it will absorb 50% of the incident radiation, reflect and transmit 25%. This method is not adaptable to the Evaporograph as presently used because of the high reflection from the metalized front surface of the membrane which makes it impossible to obtain the interference colors which are the basis for the detection of the thickness of the active material.

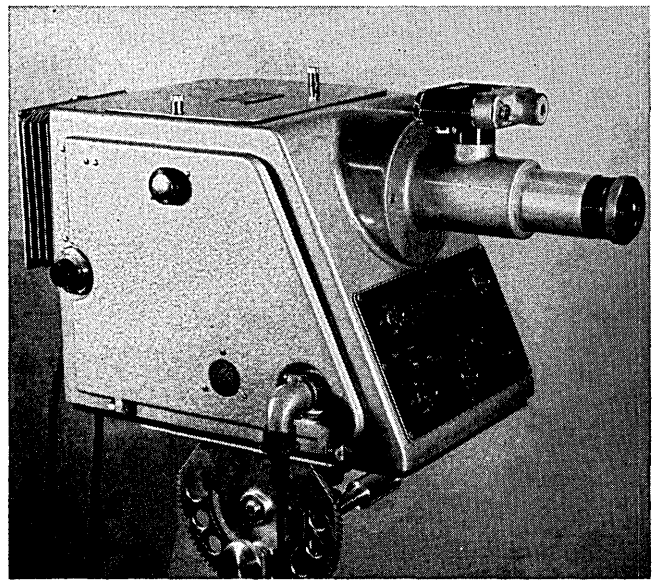

Fig. 6 Model KR-1 Evaporograph.

*Other materials.* Other investigators have used various materials such as lamp black, bismuth black, and metallic black of zinc.

### 5. *The Active Material*

The active material must condense or evaporate from the surface in such a manner that the temperature differences in the thermal image can be detected. The ideal material should have the following characteristics:

1. It should form a uniform layer on the membrane with no droplets; i.e., it should wet the membrane.
2. It should not attack the membrane or the apparatus.
3. It should not be a mixture of substances having widely different vapor pressures. Its physical characteristics should be such as to maximize the "figure of merit" derived in Eq. (16).

Two solid materials—camphor and naphthalene—have been used successfully by Czerny. The best results have been obtained with the paraffin oils, in particular with hexadecane and with the siloxane polymers. The best over-all operation has been obtained with the siloxane polymers which are available as the Dow-Corning silicone 200 fluids.

### 6. *Presentation System*

The presentation, or visual optical system of the Evaporograph, makes use of the phenomenon of light interference. Tests have been made with both monochromatic and white sources of illumination. There is little or no difference in sensitivity between the two types of sources. When a white source of illumination is used there is a definite relation between the oil film thickness and the interference color seen, as indicated in Fig. 5. Thus, there is no ambiguity as to which points of the image are warm and which are cold.

As indicated in Eq. (13), the sensitivity is directly proportional to the minimum thickness difference, $\Delta d$, of the active material that can be detected. Thus, any method of presentation which could operate with a smaller thickness difference would result in a corresponding increase in sensitivity. One type of viewing system which immediately comes to mind is phase contrast. However, this method cannot be directly applied because the reflection from the rear surface of the membrane interferes with the desired reflection from the front surface. In addition, the membrane must be extremely flat and the entire alignment of the optical system is critical.

## B. Production Evaporograph

### *1. Introduction*

The experimental work described has resulted in the development of two models of the Evaporograph.[20] The model JZ-1 Evaporograph employs a Newtonian telescope for the infrared optical system with an $f$ = 2.25 aperture and a 20 cm focal length. The angular field of view is 5°.

The model KR-1 Evaporograph uses a germanium lens optical system with aperture $f$ = 1.6 and a 7.5 cm focal length. The field of view is approximately 14°. This model is pictured in Fig. 6. The instrument can be focused down to object distances of 15 cm, resulting in a one to one image size, and features a coupled range-finder type focusing aid.

Both models have sensitivities of at least 1°C in the scene above a background temperature of 20°C and with surfaces of high emittance. With a standard parallel-bar type resolution chart having a background temperature of 20°C and a "line" temperature of 30°C, the maximum resolution is ten lines per millimeter on the membrane.

### *2. Model KR-1 Evaporograph*

Figure 7 is a schematic diagram of the optical system of the model KR-1 Evaporograph. The infrared optical system consists of an $f$ = 1.6 germanium lens with a 7.5 cm focal length. This is equipped with an iris diaphragm and shutter, and an infrared filter to prevent unwanted reflection of the viewing illumination from the rear surface of the lens. The Evaporograph cell is located at the focal plane of the lens. The cell and germanium lens assembly are mechanically coupled to a ground glass screen and a glass lens which has the same focal length as the germanium lens. To focus the instrument, the entire assembly can be moved to one side, so that the ground glass and lens will be on the optical center line. The field of view and focus can now be visually adjusted. When the cell is returned to the operating position, the same field of view will be in focus on the membrane.

There is an incandescent lamp bulb labeled "operational clear light" which is positioned between the Evaporograph cell and the germanium lens. This lamp serves three functions:

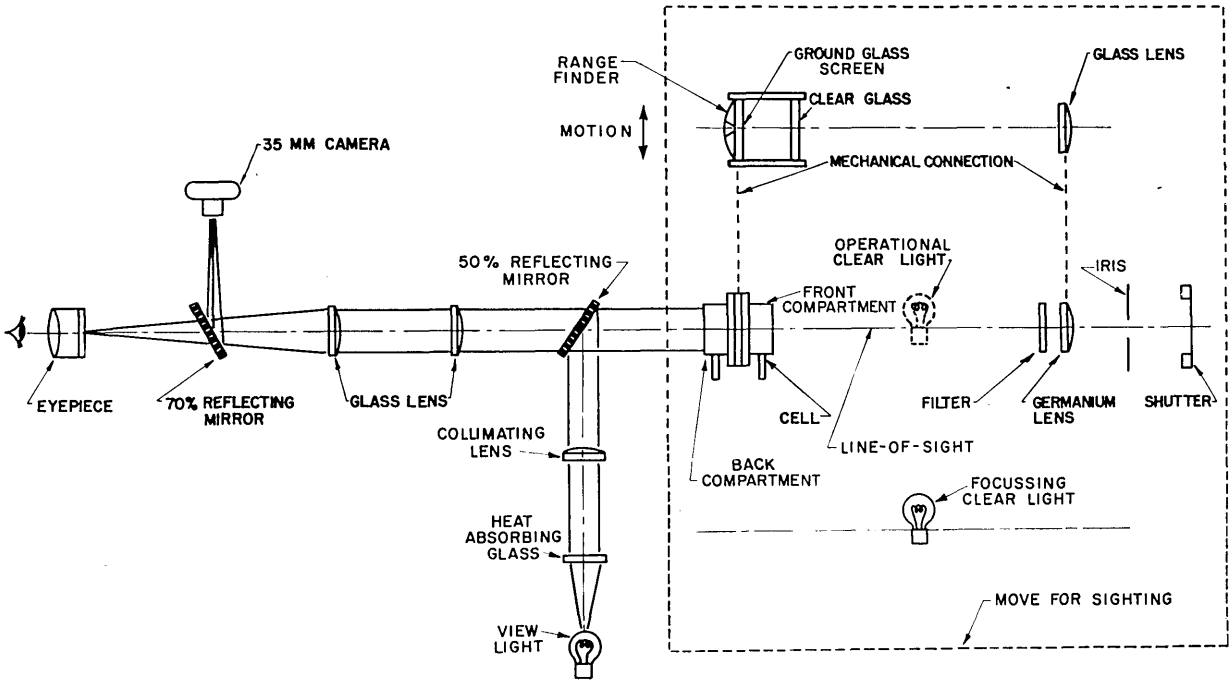


Fig. 7. Schematic diagram of the optical system of the model KR-1 Evaporograph.

1. During stand-by conditions, it floods the membrane with radiant energy, thereby warming it so that no oil will condense.

2. It also warms the front compartment of the cell, preventing any oil condensation within.

3. During operation, after the oil film has increased beyond the usable range of thickness, a few seconds' exposure to the clear light will warm the membrane and evaporate the oil so that a new imaging cycle can begin. For this purpose, the clear light is mounted on a swivel which enables the operator to swing it in and out of the optical path as desired.

The visual optical system consists of an automotive-type lamp placed at the focus of the collimating lens. Parallel light from this lens is reflected from the 50% mirror to the membrane in the cell. The reflection from the membrane then passes through the 50% mirror to a pair of lenses which form an image of the membrane at the eyepiece and at the film plane of the camera.

### 3. *Operation*

The construction of the Evaporograph cell as shown in Fig. 2 is quite different from that of Czerny. In Czerny's model, the oil is contained in a small reservoir in which an electric heater is immersed. The reservoir can be rotated into position in front of the membrane. When desired, the reservoir is positioned and the heater is turned on. Oil then evaporates from the heater and deposits on the membrane in much the same manner as an aluminum coating is applied to a mirror. When the desired film thickness is attained as indicated by the interference colors, the heater is turned off and the reservoir swung away from the membrane. The thermal image can now be seen as the oil layer evaporates from the membrane.

In the cell construction used here, the oil is contained within an absorbent layer on the inner periphery of the cell wall. The entire wall is warmed by the heater which slips over the outside. This heats the oil, raising the vapor pressure to the point where oil will begin to condense upon the surface of the membrane. Two methods of operation are now possible:

1. The scene can be focused on the membrane. Then, as soon as the clear light is removed from the front of the cell, condensation of oil on the membrane will begin. The rate of condensation at any point will depend upon the irradiance at that point, so that an oil film will build up having thickness variations which reproduce the thermal image on the membrane. This method of operation should appropriately be termed the Condensograph method, since the image is formed as the oil is condensing upon the membrane.

2. Conversely, if there is sufficient irradiance at the membrane, the shutter can be closed and the clear light removed, allowing an oil film to form on the membrane. When it has reached the desired thickness, the shutter is opened and the thermal image will now cause the film to evaporate at a rate depending upon the local irradiance. Thus, the image will become visible. This is the true Evaporograph method of operation.

Both methods can be used with this cell design and each has its own advantages. In general, for scene temperatures below 50°C, the Condensograph method is preferred, while for higher temperatures, the Evaporograph method must be used.

### 4. *Applications*

The Evaporograph has proved to have many applications, only a few of which can be illustrated here. There has been great interest by the medical profession[21] in the use of thermal imaging for diagnostic purposes. The possibilities are indicated in Fig. 8, which shows a girl holding a cold glass of water. The detail apparent in the skin, clothing, hair and glasses demonstrate the results that can be obtained. Figure 9 is the image of a seated man afflicted with phlebitus of the left leg. The temperature difference between the two legs is obvious.

Figure 10 shows the image of Boston Harbor as seen from downtown Boston at night. The large smoke stack in the foreground is unmistakable, as well as two smaller stacks to the right. Careful examination shows that Logan Airport can be seen against Boston Harbor in the background. This is located at a distance of approximately eight miles.

Figure 11 depicts an unusual application in which a filament of Fiberglas is examined as it is being drawn from a platinum nozzle. The dark streak extending out of the picture is the filament of glass emerging from the cone-shaped molten glass visible as it issues from the nozzle. The light irregular band above the cone is a deposit of glass which has congealed on the outside surface of the nozzle. The nozzle itself appears cool because of the low emissivity of the platinum. By means of the techniques already described it was possible to measure the temperature gradient along the Fiberglas filament and cone.

Other applications include the following:

1. Nondestructive testing of bonds and other joints.

2. Thermal studies of process equipment, such as heat exchangers.

3. Wind tunnel temperature observation.

4. Observation of electronic assemblies to locate hot spots.

5. Observation of in-service blast furnaces to locate dangerously thin areas in the furnace lining or the formation of scabs within.

6. Observation of high power switch gear and power distribution systems to locate faulty joints or contacts before actual burnout occurs.

Fig. 8. Evaporograph image of a girl holding a glass of cold water.

Fig. 9. Evaporograph image of a seated man afflicted with phlebitus of the left leg.

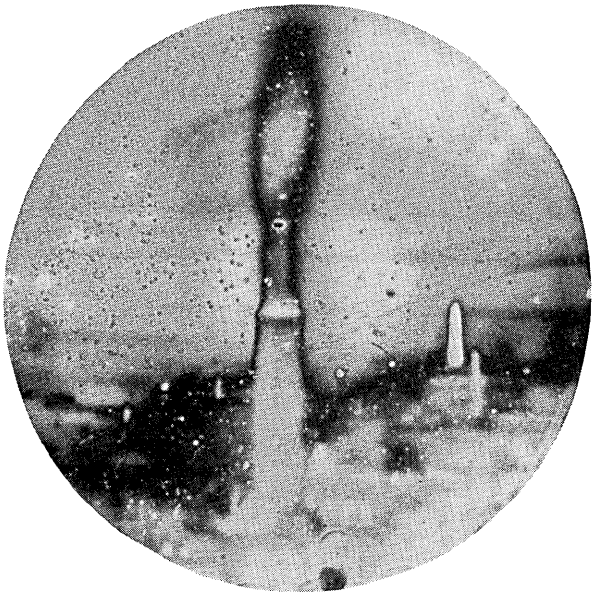

Fig. 10. Evaporograph image of Boston Harbor at night.

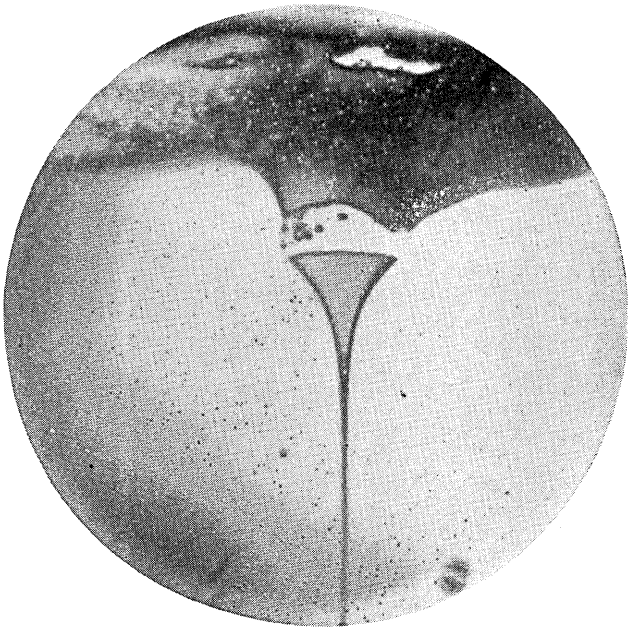

Fig. 11. Evaporograph image of a filament of Fiberglas as it is being drawn.

7. Inspection of infrared optical materials and systems.

## Conclusions

The Evaporographic method of thermal imaging is an outstanding example of the application of simple principles to obtain a useful device. Its very simplicity allows the construction of a small, light-weight device capable of operating under extreme environmental conditions. The ideal design of the Evaporograph awaits the development of more permanent membranes and of a sealed-off cell that would require no vacuum pump. A different presentation system that could operate with smaller differences in oil thickness would result in a corresponding direct increase in sensitivity. The sensitivity at present is several orders of magnitude away from the ultimate limit imposed by the statistical nature of the evaporation (or condensation) process.

Many persons have contributed to the development of the Evaporograph as described herein. In particular, the authors wish to recognize the work of A. P. DiMattia who has assisted in all phases of the development, of Mrs. J. Gillingham for many hours spent in testing and evaluating oils, blacks, and membranes, and of Mrs. W. Hampton who has mastered the art of membrane making.

## References

1. W. K. Weihe, Proc. Inst. Radio Engrs. **47**, 1593 (1959).
2. W. Herschel, Phil. Trans. Roy. Soc. London **Pt. II**, 90, 225 (1800).
3. J. F. W. Herschel, Phil. Trans. Roy. Soc. London **131**, 52 (1840).
4. M. Czerny, Z. Physik **53**, 1 (1929).
5. M. Czerny and P. Mollet, Z. tech. Physik **18**, 582 (1937).
6. D. Z. Robinson, A. P. DiMattia, and G. W. McDaniel, J. Opt. Soc. Am. **47**, 340 (1957) (Abstract only).
7. C. Hilsum and W. R. Harding, Infrared Phys. **1**, 67 (1961).
8. M. Garbuny, T. P. Vogl, and J. R. Hansen, J. Opt. Soc. Am. **51**, 261, (1961).
9. L. Harris and R. T. McGinnies, J. Opt. Soc. Am. **38**, 582 (1948).
10. I. Langmuir, Phys. Rev. **2**, 329 (1913).
11. I. Langmuir and G. M. J. Mackay, Phys. Rev. **4**, 377 (1914).
12. S. Glasstone, *Textbook of Physical Chemistry*, 2nd ed., p. 443. Van Nostrand, New York, 1946.
13. H. Kubota, T. Ara, and H. Saito, J. Opt. Soc. Am. **41**, 537 (1951).
14. W. R. J. Brown and D. L. MacAdam, J. Opt. Soc. Am. **39**, 808 (1949).
15. M. Czerny and P. Mollet, Z. Physik **108**, 85 (1937).
16. L. Harris and E. A. Johnson, Rev. Sci. Instr. **4**, 454 (1933).
17. G. Hass and M. E. McFarland, J. Appl. Phys. **21**, 435 (1950).
18. K. Strohmaier, Z. Naturforsch. **6a**, 508 (1951).
19. L. N. Hadley and D. M. Dennison, J. Opt. Soc. Am. **37**, 451 (1947).
20. D. Z. Robinson, G. W. McDaniel, and A. P. DiMattia, U.S. Patent 2,855,522.
21. R. N. Lawson, Can. Services Med. J. **13**, 517 (1957).

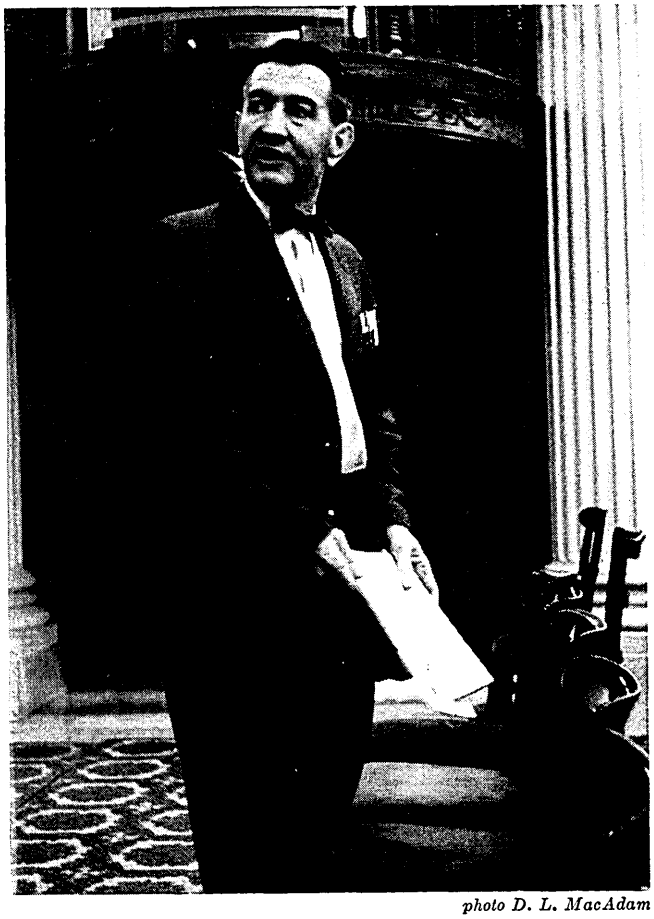

*photo D. L. MacAdam*

The new Treasurer of the Optical Society of America Archie I. Mahan and author of a paper on refraction in the July issue.

Participating in the July 1961 ICO London sessions are G. Novarski *Paris*, A. N. Other, D. Marquis *Cape Canaveral*, Stanley S. Ballard *Fla.*, P. Fleury *Paris*, and W. Wolfe *IRIA*.

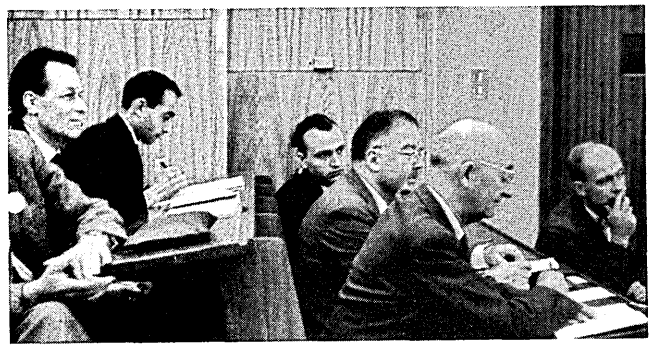

J. Dyson *London*, R. E. Hopkins *Rochester*, and two other participants in the July 1961 London ICO Meeting.